Advanced Physical Research
Vol.8, No.1, 2026, pp.5-13
https://doi.org/10.62476/apr.8105

THE PRESSURE-INDUCED STRUCTURAL PHASE TRANSITION IN $LaCo_{0.5}Mn_{0.5}O_3$ MANGANITE

L.H. Khiem[1], S.E. Kichanov[2], O.N. Lis[2*], N.T. Nguyen[2,3,4], E.V. Lukin[2], D.P. Kozlenko[2], A.I. Bayramova[5], T.P. Hoang[6,7], N.T. Dang[6,7]

[1]Institute of Physics, Vietnam Academy of Science and Technology, Hanoi, Vietnam
[2]Frank Laboratory of Neutron Physics, Joint Institute for Nuclear Research, Dubna, Russia
[3]Faculty of Electronics, Electrical Engineering and Material Technology, University of Sciences, Hue University, Hue, Vietnam
[4]Institute of Oceanography, Vietnam Academy of Science and Technology, Nha Trang, Vietnam
[5]Azerbaijan University of Architecture and Construction, Baku, Azerbaijan
[6]Institute of Research and Development, Duy Tan University, Danang, Vietnam
[7]Faculty of Environmental and Natural Sciences, Duy Tan University, Danang, Vietnam

Abstract. The structural and vibrational properties of $LaCo_{0.5}Mn_{0.5}O_3$cation-disordered manganite have been studied using *X*-ray diffraction and Raman spectroscopy at pressures up to 25 GPa. The application of high pressures above 5 GPa leads to a gradual structural phase transition from an orthorhombic crystal structure with *Pnma* symmetry to *Imma* one, accompanied by anomalies in the behaviour of lattice parameters, unit cell volumes, and some Raman modes under pressure. Pressure dependencies of structural parameters and frequencies of Raman modes for the observed phases of the $LaCo_{0.5}Mn_{0.5}O_3$ manganese oxide were obtained.

Keywords: *X*-ray diffraction, Raman spectroscopy, high pressure, phase transition, perovskite oxides.
Corresponding author: O.N. Lis, Frank Laboratory of Neutron Physics, Joint Institute for Nuclear Research, Dubna, Russia, e-mail: *lisa_9477@mail.ru*
Received: 14 August 2025; Revised: 17 October 2025; Accepted: 24 November 2025; Published: 18 February 2026.

1 Introduction

Studying the structure and phase transitions of condensed matter is of great importance. The results obtained from this research help explain the physical properties that develop within them. Studying the crystals and thin films of functional materials determines their potential applications (Kitano et al., 2013; Jabarov et al., 2022). Strongly correlated perovskite oxides continue to be the subject of extensive research due to their variety of catalytic (Yamada et al., 2017; Polo-Garzon & Wu, 2018), pyroelectric (Serralta-Macías et al., 2021), piezoelectric (Shohag et al., 2024), ferroelectric (Cong et al., 2018), dielectric (Yousif et al., 2021), resistivity (Kozuka et al., 2015), superconductivity properties (Zhou et al., 2018), and the potential cross-couplings between these responses (Zeng et al., 2020). These materials have prospects potential technical applications as promising candidates for novel electronic devices (Zeng et al., 2020; Jia et al., 2023). In addition, perovskite magnetic oxides are characterized by a rich range of magnetic phases from ferromagnetic and antiferromagnetic to unique non-collinear or incommensurate magnetic states (Mandal et al., 2007).

In perovskite manganese oxides, the interplay between magnetic, transport, and electronic properties is based on a delicate balance between the ferromagnetic (FM) double exchange, promoted by charge carriers of the e_g type, and antiferromagnetic (AFM) super-exchange interactions between localized magnetic moments t_{2g} that are tuned by lattice distortions and orbital degrees of freedom (de Gennes, 1960; Dagotto et al., 2001; Coey et al., 1999). Well-studied undoped $LaMnO_3$ is a classic example of a Jahn-Teller (JT) system (Pavarini et al., 2010; Rodriguez et al., 1998), where cooperative JT structural distortions remove the degeneracy of the half-filled e_g orbital of Mn^{3+} ions, leading to the formation of antiferrodistortive long-range orbital ordering and an AFM insulating ground state (Rodriguez et al., 1998). With the introduction of holes into mixed valency $R_{1-x}A_xMnO_3$ systems, the long-range JT structural distortions are gradually suppressed and the FM metallic state appears when $0.2 < x < 0.5$ (Basak et al., 2001). On the other hand, the doping of the manganese site with transition metal ions provokes changing of double exchange interactions (Ghosh et al., 1999). It has also been suggested that super-exchange interactions between different types of ions may also be responsible for cation doping. In particular, doping the manganese sublattice with cobalt ions with different spin-states contributes to the formation of intriguing magnetic properties (Troyanchuk et al., 2000). In the ideal fully ordered structure of cobalt-doped manganites the positions of Co^{2+} and Mn^{4+} ions are swapped (Sazonov et al., 2006). A super-exchange magnetic interaction between cobalt and manganese ions results in the long-range ferromagnetic FM order (Pollert et al., 2003). The cation disordering in the perovskite manganite oxides triggers an increase in $Mn^{4+} - O - Mn^{4+}$ and $Co^{2+} - O - Co^{2+}$ double exchange interactions. Formation of FM ordering is shown in $LaCo_{0.5}Mn_{0.5}O_6$ at $T_C = 210K$ with comparable low values of ordered magnetic moments (Khiem et al., 2025).

An important insight into the relationship between the competing factors discussed above and their particular role in formation of magnetoelectric properties of perovskite compounds can be given by high pressure studies (Kozlenko et al., 2011, 2023; Belozerova et al., 2021). There is an exploration of the response of physical properties to the reduction of interatomic distances and the mediation of relevant interactions. High pressure generally leads to metallization of manganese oxide owing to the broadening of charge carrier bandwidth W and the closure of the energy gap in the band structure (Loa et al., 2001). Raman spectroscopy reveals a peculiar behavior of the JT mode of MnO_6 octahedra characterized by a rapid increase in wavenumber up to $\sim 7GPa$ and its subsequent weak dependence on pressure up to 14 GPa (Sacchetti et al., 2008). This allows for anisotropic compression of oxygen octahedral structures. In the case of cation-disordered manganates, high pressure application can significantly affect the different responses of two octahedral structures around manganese and cobalt ions. However, in cation-disordered perovskites, the effect of high pressure on the crystal structure remains unclear, but it is an important factor in understanding the evolution of the magnetic properties of such manganates under pressure. For further insight into the structural and vibrational properties of $LaMn_{0.5}Co_{0.5}O_3$ at high pressure, we performed X-ray and Raman spectroscopy measurements in the pressure range up to 25 GPa.

2 Experimental

As previously described (Khiem et al., 2025), the synthesis of $LaCo_{0.5}Mn_{0.5}O_3$ polycrystalline samples was accomplished using a conventional sol-gel method. The starting materials were high-purity lanthanum nitrate hexahydrate ($La(NO_3)_3 \cdot 6H_2O$), cobalt sulfate heptahydrate ($CoSO_4 \cdot 7H_2O$), and manganese nitrate tetrahydrate ($Mn(NO_3)_2 \cdot 4H_2O$). These precursors were mixed in the correct proportions to create a uniform solution. Citric acid was added as a chelating agent, and the reaction was conducted in an alkaline environment. The solution was continuously stirred and gradually heated up to 450 °C to facilitate gel formation and subsequent decomposition. The resulting gel was ground into a fine powder and then subjected to annealing

at 1150 $^{\circ}C$ for 12 hours to produce the final product.

The X-ray diffraction (XRD) experiments were performed using the SAXS/WAXS XEUSS 3.0 system (produced by Xenocs SAS in Grenoble, France) with the Dectris Eiger 2R 500K detector. The wavelength of Mo $K\alpha$ radiation was $\lambda = 0.7115$. The XRD data were analyzed using the software package FullProf (Rodriguez, 1993).

Raman spectra at high pressures and ambient temperature were obtained using a Confotec MR200 spectrometer (produced by SOL Instruments GmbH, Augsburg, Germany) with a wavelength excitation of 532 nm from a diode-pumped solid-state laser, 1200-mm grating, a confocal hole of 100 μm, and a $\times 20$ objective. The laser power was 17 mW. An absorption coefficient of the studied material for laser excitation wavelengths in the range 488–633 cm^{-1} is relatively low, and the local heating effects should be negligible.

A Boehler-Almax plate-type diamond anvil cell (DAC) was used in the experiments at high pressures up to 25 GPa. Diamonds with culets of 300 μm were selected. The sample was loaded into a hole of 150 μm diameter made in a rhenium gasket, indented to approximately 30 μm thickness. The pressure was determined using the ruby fluorescence technique at three ruby balls: one in the center of the gasket and two others close to the boarders. Accuracy of the pressure determination at each ruby was on the limit of 0.1 GPa, and no pressure-transmitting medium was used to avoid its interaction with the studied material, improving background conditions for Raman spectroscopy experiments.

3 Results

3.1 X-ray diffraction

The X-ray diffraction patterns of $LaCo_{0.5}Mn_{0.5}O_3$ measured at selected pressures and ambient temperature, are shown in Figure 1.

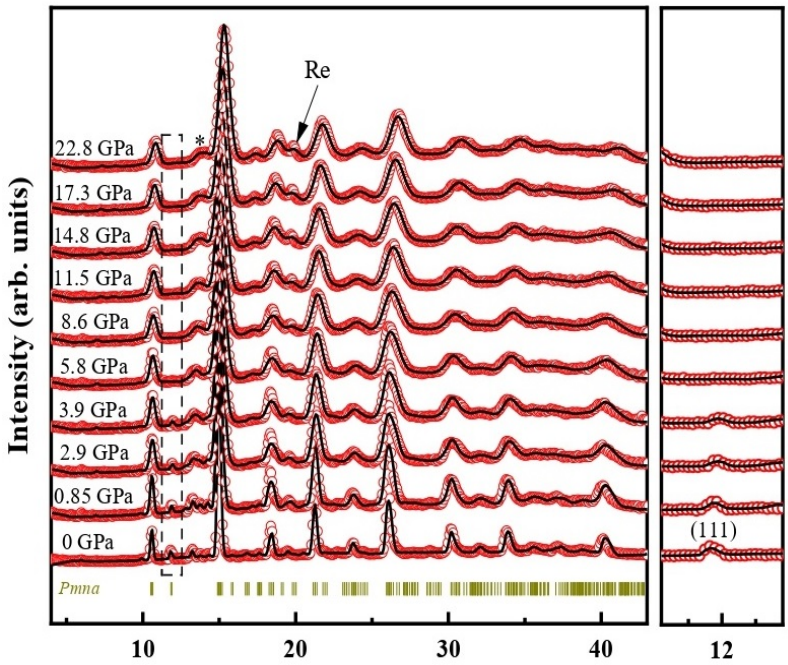

Figure 1: The XRD patterns of $LaCo_{0.5}Mn_{0.5}O_3$ measured at selected pressures. The experimental points and calculated profiles obtained using the Rietveld method are presented. The ticks below represent the calculated positions of the diffraction peaks corresponding to the *Pnma* phase at $P = 0.1GPa$. Additional peaks from the gasket material are denoted as Re and $*$. The enlarged parts of the XRD patterns (highlighted with a dotted rectangle) are presented, showing the evolution of the (111) diffraction peak with pressure.

Under ambient conditions, $LaCo_{0.5}Mn_{0.5}O_3$ has an orthorhombically distorted perovskite crystal structure of *Pnma* symmetry and lattice parameters of $a = 5.472(2)$ A, $b = 7.718(3)$ A, $c = 5.475(2)$ A. These values are in good agreement with the previous data (Dass & Goodenough, 2003; Khiem et al., 2025; Selmi et al., 2022). In the orthorhombic phase, the lattice parameters correspond to perovskite unit cell as $a \sim \sqrt{2}a_p, b \sim 2a_p$, and $c \sim \sqrt{2}a_p$, where a_p is the parameter of the perovskite cubic phase. In orthorhombic phase, Co and Mn ions are randomly distributed at the *6c* crystallography site.

When the pressure increases, a decrease in the intensity of the diffraction peak (111) is observed (Figure 1). At pressure $P = 5.8GPa$ this peak fully disappeared. This fact can indicate the structural phase transition into the higher symmetry phase. The phase transformation starts at $P = 3.2GPa$ and evolves over a phase coexistence in the pressure range of a few GPa. It is known that the diffraction peak (111) is forbidden for rhombohedral $R\bar{3}c$, orthorhombic *Imma*, and tetragonal *I4/mcm* space groups, which are observed in other manganites (Kozlenko et al. (2023)). It was found that the orthorhombic model with the *Imma* symmetry had the best agreement with the obtained experimental data and was chosen for the structure analysis of the high-pressure phase.

The *Pnma-Imma* structural phase transition in $LaCo_{0.5}Mn_{0.5}O_3$is accompanied by anomalies in the pressure dependence of the unit cell parameters and volume (Figure 2a and 2b). The calculated linear compressibility coefficients of the unit cell parameters $k_{ai} = -(1/a_{0i})\ (da_i/dP)|_T$ (a_i=*a, b* and *c*) are k_a=*0.0019*, k_b=*0.0020* and k_c=*0.0010* GPa^{-1} for *Pnma* phase and k_a=*0.0013*, k_b=*0.0014* and k_c= *0.0008* GPa^{-1} for high pressure phase with *Imma* space group. In the pressure range of 0 – 6 GPa, lattice compression is anisotropic with the most compressible along *b*-axis (Figure 2a). Uniaxial compression anisotropy can be characterized by the distortion parameter $s_t = b/(2ac)^{1/2}$, which is equal to 1 for the ideal cubic perovskite cell. As can be seen from Figure 2b, the s_t value for $LaCo_{0.5}Mn_{0.5}O_3$compound decreases from 0.998 to 0.989 with the pressure increase. However, in the phase transition range, there is a noticeable change in the slope of the baric dependence of the distortion parameter s_t(Figure 2b).

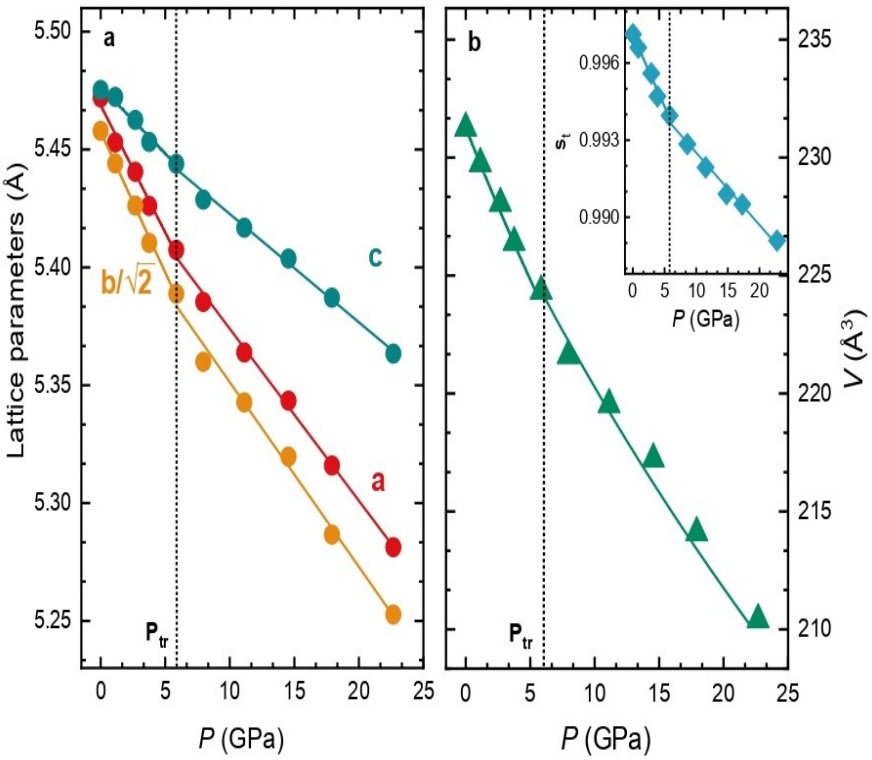

Figure 2: Pressure dependence of (a) lattice parameters and (b) unit cell volume of $LaCo_{0.5}Mn_{0.5}O_3$. The inset shows the baric dependence of distortion parameter s_t.

The volume compressibility data were fitted using the third-order Birch–Murnaghan equation of state (Birch, 1986):

$$P = \frac{3}{2}B_0\left(x^{-7/3} - x^{-5/3}\right)\left[1 + \frac{3}{4}(B' - 4)(x^{-2/3} - 1)\right] \quad (1)$$

where $x = V/V_0$ is the relative volume of unit cell and V_0 is the unit cell volume at $P = 0$; B_0 and B' are the bulk modulus $B_0 = -V\ (dP/dV)_T$ and its pressure derivative $B' = (dB_0/dP)_T$. The calculated values for the *Pnma* orthorhombic phase of $LaCo_{0.5}Mn_{0.5}O_6$ are $B_0 = 167(6)$ GPa, $B' = 4(1)$ and $B_0 = 197(6)$ GPa, $B' = 4(1)$ for the high-pressure phase with the *Imma* space group. The values of the bulk modulus are comparable to the values obtained for similar manganite compounds $Pr_{0.7}Ba_{0.3}MnO_3$ (B_0=144(5)GPa), $Pr_{0.7}Sr_{0.3}MnO_3$ (B_0=120(5) GPa for *Pnma* phase and B_0=168(5) GPa for *Imma* phase, respectively) (Dang et al., 2013), $La_{0.7}Sr_{0.3}MnO_3$ (B_0=167(5) GPa) (Kozlenko et al., 2004), $La_{0.75}Ca_{0.25}MnO_3$ (B_0=178 GPa) (Kozlenko et al., 2007), $LaMn_{0.7}Ga_{0.3}O_3$ (B_0=160 GPa) (Malavasi et al., 2010).

It should be noted that both the *Pnma* and *Imma* phases have similar superstructures with respect to the ideal perovskite subunit, but they differ mainly in the tilt system of the oxygen octahedra (Kozlenko et al., 2023). While in the *Pnma* phase the tilts of $Mn(Co)O_6$ octahedra around (010) and (101) axes are present ($a^-b^+a^-$ tilt system in Glazer notation), in the *Imma* phase tilts around (101) axis are allowed only ($a^-b^0a^-$ tilt system). And these subtle effects can only be verified in Raman spectroscopy experiments.

3.2 Raman spectroscopy

Raman spectra of $LaCo_{0.5}Mn_{0.5}O_3$ measured at different pressures are shown in Figure 3. They exhibit two strong peaks located at 490 and 650 cm^{-1} (Figure 3a). In comparison to $LaMnO_3$and other manganite compounds with the JT distortions, those peaks correspond to the bending vibration mode (AS) with the A_g symmetry and to the symmetrical stretching vibration mode (SS) with the B_{2g} symmetry, respectively. Over the studied pressure range up to 25 GPa, is an almost linear increase in the frequency of the observed modes (Figure 3c), while an anomaly on the pressure dependence of the AS mode frequency is detected at pressure above $\sim$ 4.2 GPa. Also, at pressures above 5.5 GPa, an additional weak Raman peak appeared at$\sim$ 390 cm^{-1}. It corresponds to a bending deformation (BD) mode of $Mn(Co)O_6$ octahedra with B_{3g} symmetry. The *Pnma- Imma* phase transition at $P \sim 5.5$ GPa is related to tilting of $Mn(Co)O_6$ octahedra and it weakly affects the Mn-O and Co-O distances, controlling the SS mode frequency.

Interestingly, when the manganese sublattice is doped with cobalt ions in $LaCo_{0.5}Mn_{0.5}O_3$, no expected suppression of static cooperative JT distortions was detected. In addition, a splitting of the SS mode peak into two peaks is expected. We checked this statement by studying the pressure dependence of the widths of the Raman lines for AS and SS modes (Figure 3d). It is clearly seen that if the full width at half maximum (FWHM) of the AS vibrational mode does not change significantly under pressure, there is a noticeable decrease in the width of the SS mode before the phase transition and a gradual widening with further increasing pressure. We assumed that this is related to a difference in the average compressibility of the Mn-O and Co-O distances in both the *Pnma* and *Imma* phases.

Interestingly, the JT mode in the $LaCo_{0.5}Mn_{0.5}O_3$ compound does not disappear at high pressure, as was observed in the undoped $LaMnO_3$ compound (Kozlenko et al., 2023). This is due to the strong local antiferrodistortive JT coupling between nearest-neighbors octahedra. These are similar local JT-distorted regions with a short-range orbital order and coupling, but are likely with a larger correlation length compared to high-temperature phases of $LaMnO_3$. The character of JT distortion can be modified from a long-range to a local one due to doping and pressure application. In turn, the change in the JT structural distortion determines the presence of an orbital order in manganites, which determines the A-type antiferromagnetic state (Kozlenko et al., 2011, 2023). The local incoherent JT lattice distortions, of a static or dynamic

nature, and related electron-phonon coupling effects, combined with inner strains caused by cation disordering in cation disordering effects in the $LaCo_{0.5}Mn_{0.5}O_3$, may lead to the formation of the nanoscopic or mesoscopic A-type AFM regions in the initial FM matrix (Kozlenko et al., 2023). However, this requires conducting neutron diffraction experiments at high pressures.

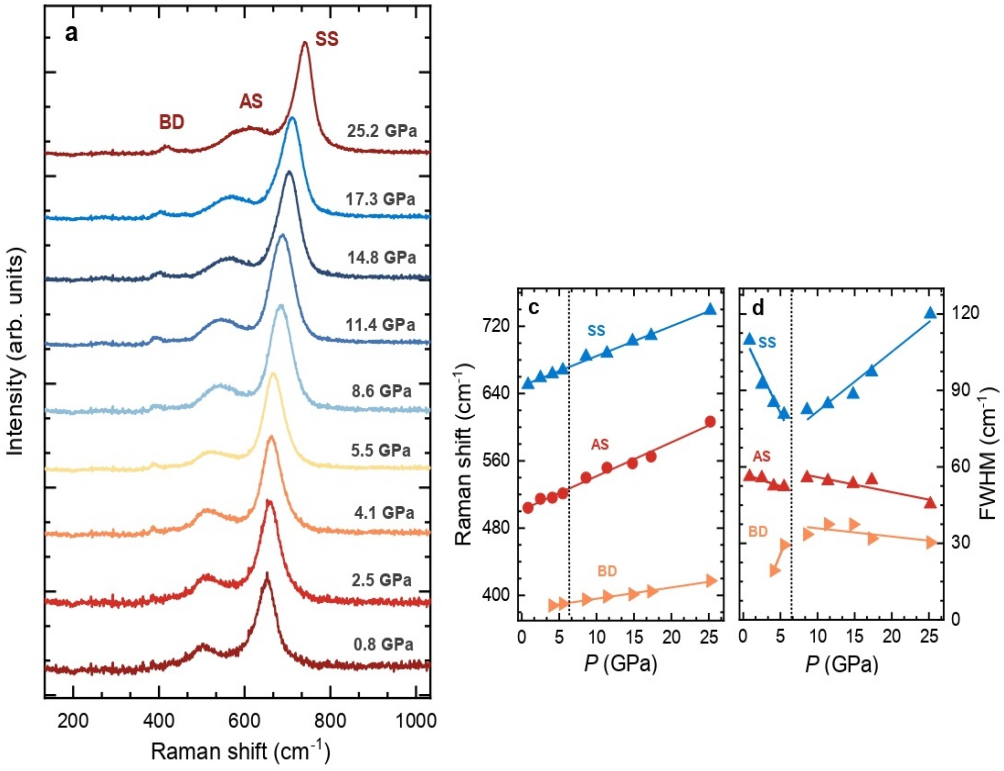

Figure 3: The Raman spectra of $LaCo_{0.5}Mn_{0.5}O_3$ measured at selected pressures and ambient temperature and the enlarged part of Raman spectra (b) for the high pressure Imma phase obtained at $P = 8.6$ GPa. Pressure dependencies of the observed Raman modes (c) and their Full width at half maximum (FWHM) (d) of $LaCo_{0.5}Mn_{0.5}O_3$.

4 Conclusion

A comprehensive high-pressure study of the cation-disordered perovskite $LaCo_{0.5}Mn_{0.5}O_3$ has been performed using X-ray diffraction and Raman spectroscopy up to 25 GPa. The results revealed a pressure-induced structural phase transition from the initial orthorhombic *Pnma* phase to the *Imma* phase at $P \sim 5$ GPa. This structural phase transition is accompanied by the appearance of a new Raman-active mode associated with bending vibrations of the $(Mn/Co)O_6$ octahedra and by the anomalous in the pressure dependence of FWHM linewidths of observed vibrational modes. Based on experimental data and previous results, it is expected that the gradual suppression of FM order in $LaCo_{0.5}Mn_{0.5}O_3$ will occur, mediated by changes in octahedral tilting and anisotropic lattice compression.

5 Acknowledgements

This work has been supported by the joint grants of the Russian Science Foundation, RSF No:24-42-04002, `https://rscf.ru/project/24-42-04002/` and the grant of the Vietnam Academy of Science and Technology, QTRU06.07/24-26.

References

Basak, S., Chaudhuri, I. & Ghatak, S.K. (2001). Effect of strain on the transport properties of THE manganite. *International Journal of Modern Physics B, 15*(27), 3551-3558. https://doi.org/10.1142/S021797920100735X

Belozerova, N.M., Kichanov, S.E., Jirák, Z., Kozlenko, D.P., Kaman, O., Lukin, E.V & Savenko, B.N. (2021). The crystal and magnetic structure of nanostructured manganite La0.53Sr0.47MnO3 at high pressure. *Materials Chemistry and Physics*, 262, 124310. https://doi.org/10.1016/j.matchemphys.2021.124310

Birch, F. (1986). Equation of state and thermodynamic parameters of NaCl to 300 kbar in the high-temperature domain. *Journal of Geophysical Research*, 91, 4949-4954. https://doi.org/10.1029/JB091iB05p04949

Coey, J.M.D., Viret, M. & von Molnár, S. (1999). *Mixed-valence manganites. Advances Physics*, *48*, 167-293. https://doi.org/10.1080/000187399243455

Cong, J., Zhai, K., Chai, Y., Shang, D., Khalyavin, D.D., Johnson, R.D., Kozlenko, D. P., Kichanov, S.E., Abakumov, A.M., Tsirlin, A.A., Dubrovinsky, L., Xu, X., Sheng, Z., Ovsyannikov, S.V & Sun, Y. (2018). Spin-induced multiferroicity in the binary perovskite manganite Mn2O3.*Nature Communications, 9,* 2996. https://doi.org/10.1038/s41467-018-05296-0

Dagotto, E., Hotta, T. & Moreo, A. (2001). Colossal magnetoresistant materials: the key role of phase separation. *Physics Reports, 344*, 1-153. https://doi.org/10.1016/S0370-1573(00)00121-6

Dang, N.T., Kozlenko, D.P., Kichanov, S.E., Dubrovinsky, L.S., Jirák, Z., Levin, D.M., Lukin, E.V. & Savenko, B.N. (2013). Structural and magnetic phase transitions occurring in Pr0.7Sr0.3MnO3 manganite at high pressures. *JETP Letters, 97*, 540-545. https://doi.org/10.1134/S0021364013090075

Dass, R.I., Goodenough, J.B. (2003). Multiple magnetic phases of $La_2CoMnO6 - (0 <\sim<\sim 0.05)$. *Physical Review B, 67*, 014401.

de Gennes, P.G. (1960). Effects of double exchange in magnetic srystals. *Physical Review, 118*, 141-154. https://doi.org/10.1103/PhysRev.118.141

Ghosh, K., Ogale, S.B., Ramesh, R., Greene, R.L., Venkatesan, T., Gapchup, K.M., Bathe, R. & Patil, S.I. (1999). Transition-element doping effects in La0.7Ca0.3MnO3. *Physical Review B, 59*, 533-537. https://doi.org/10.1103/PhysRevB.59.533

Jabarov, S.H., Ibrahimova, S.I., Hajiyeva, F.V., Huseynov, E.M., Aliyev, Y.I. (2022). Structural, vibrational, and dielectric properties of CuInZnSe3 chalcogenide compound. *Arabian Journal for Science and Engineering*, *47*(6), 7817-7823. https://doi.org/10.1007/s13369-022-06745-1

Jia, Z., Cheng, C., Chen, X., Liu, L., Ding, R., Ye, J., Wang, J., Fu, L., Cheng, Y. & Wu, Y. (2023). Applications of all-inorganic perovskites for energy storage. *Materials Advances*, *4*, 79-104. https://doi.org/10.1039/D2MA00779G

Khiem, L.H., Kichanov, S.E., Lis, O.N., Nguyen, N.T., Lukin, E.V, Vershinina, T.N., Kozlenko, D.P., Golosova, N.O., Truong-Tho, N., Dang, N.T. & Hoang, T.P. (2025). The crystal and magnetic structure of the cation-disordered perovskites LaCo0.5Mn0.5O3 and YCo0.5Mn0.5O3. *International Journal of Modern Physics B, 39*, 2550239. https://doi.org/10.1142/S021797922550239X

Kitano, A., Shim, Y.G., Wakita, K., Khalilova, Kh., Mamedov, N., Bayramov, A., Huseynov, E., Hasanov, I. (2013). Optical characterization of non-annealed CdS:O films for window layers in solar cells. *Physica Status Solidi (C) Current Topics in Solid State Physics, 10*, 1107-1110. https://doi.org/10.1002/pssc.201200834

Kozlenko, D.P., Chan, T.A., Kichanov, S.E., Trukhanov, A.V, Trukhanov, S.V. & Savenko, B.N. (2011). Study of crystal and magnetic structures of manganite Pr0.7Ba0.3MnO3 at high pressure. *Physics of Particles and Nuclei Letters, 8,* 1063-1065. https://doi.org/10.1134/S1547477111100098

Kozlenko, D.P. Goncharenko, I.N., Savenko, B.N. & Voronin, V.I. (2004). High pressure effects on the crystal and magnetic structure of La0.7Sr0.3MnO3. *Journal of Physics: Condensed Matter, 16,* 6755. https://doi.org/10.1088/0953-8984/16/37/011

Kozlenko, D.P., Lukin, E.V, Kichanov, S.E., Jirák, Z., Golosova, N.O. & Savenko, B.N. (2023). High-pressure evolution of the magnetic order in LaMnO3. *Physical Review B, 107*, 144426. https://doi.org/10.1103/PhysRevB.107.144426

Kozlenko, D.P., Ovsyannikov, S.V, Shchennikov, V.V, Voronin, V.I. & Savenko, B.N. (2007). Thermoelectric properties of La0.75Ca0.25MnO3 manganite at ultrahigh pressures up to 20 GPa. JETP Letters, 85, 203-207. https://doi.org/10.1134/S0021364007040042

Kozuka, H., Ohbayashi, K. & Koumoto, K. (2015). Electronic conduction in La-based perovskite-type oxides. *Science and Technology of Advanced Materials, 16,* 026001. https://doi.org/10.1088/1468-6996/16/2/026001

Loa, I., Adler, P., Grzechnik, A., Syassen, K., Schwarz, U., Hanfland, M., Rozenberg, G.K., Gorodetsky, P. & Pasternak, M.P. (2001). Pressure-induced quenching of the Jahn-Teller distortion and insulator-to-metal transition in LaMnO3. *Physical Review Letters, 87*, 125501. https://doi.org/10.1103/PhysRevLett.87.125501

Malavasi, L., Baldini, M., di Castro, D., Nucara, A., Crichton, W., Mezouar, M., Blasco, J. & Postorino, P. (2010). High pressure behavior of Ga-doped LaMnO3: a combined X-ray diffraction and optical spectroscopy study. *Journal of Materials Chemistry, 20*, 1304-1311. https://doi.org/10.1039/B914975A

Mandal, T.K., Abakumov, A.M., Hadermann, J., Van Tendeloo, G., Croft, M. & Greenblatt, M. (2007). Synthesis, crystal structure, and magnetic properties of Sr1.31Co0.63Mn0.37O3: a derivative of the incommensurate composite hexagonal perovskite structure. *Chemistry of Materials, 19,* 6158-6167. https://doi.org/10.1021/cm071840g

Pavarini, E. & Koch, E. (2010). Origin of Jahn-Teller distortion and orbital order in LaMnO3. *Physical Review Letters, 104,* 86402. https://doi.org/10.1103/PhysRevLett.104.086402

Pollert, E., Hejtmánek, J., Jirák, Z., Knìžek, K. & Marysko, M. (2003). Influence of Co doping on properties of Pr0.8Na0.2Mn(1-y)CoyO3 perovskites. *Journal of Solid State Chemistry, 174,* 466-470. https://doi.org/10.1016/S0022-4596(03)00311-6

Polo-Garzon, F., Wu, Z. (2018). Acid - base catalysis over perovskites: a review. *Journal of Materials Chemistry A, 6*, 2877-2894. https://doi.org/10.1039/C7TA10591F

Rodríguez-Carvajal, J. (1993). Recent advances in magnetic structure determination by neutron powder diffraction. *Physica B: Condensed Matter*, 192, 55-69. https://doi.org/10.1016/0921-4526(93)90108-I

Rodriguez-Carvajal, J., Hennion, M., Moussa, F., Moudden, A.H., Pinsard, L. & Revcolevschi, A. (1998). Neutron-diffraction study of the Jahn-Teller transition in stoichiometric LaMnO3. *Physical Review B, 57,* R3189-R3192. https://doi.org/10.1103/PhysRevB.57.R3189

Sacchetti, A., Corridoni, T., Arcangeletti, E. & Postorino, P. (2008). High pressure Raman study of La1-xCaxMnO3-δ manganites. *The European Physical Journal B, 66,* 301-305. https://doi.org/10.1140/epjb/e2008-00441-1

Sazonov, A.P., Troyanchuk, I.O., Kozlenko, D.P., Balagurov, A.M. & Sikolenko, V.V (2006). Magnetic ordering in the $Nd_2CoMnO_{6+\delta}$ perovskite system. *Journal of Magnetism and Magnetic Materials, 302,* 443-447. https://doi.org/10.1016/j.jmmm.2005.10.004

Selmi,R., Cherif, W., Sarabando, A.R., Ferreira, N.M. & Ktari, L. (2022). Crystal structure and magnetic properties in B-site-disordered La1.75Ca0.25MnMO6 (with $M = Ti$ and Fe) double perovskites. Journal of Superconductivity and Novel Magnetism, 35, 1195-1206. https://doi.org/10.1007/s10948-022-06174-z

Serralta-Macías, J.J., Calderón-Piñar, F., García Zaldivar, O., Olguín, D. & Yáñez-Limón, J.M. (2021). Structural, ferroelectric, pyroelectric, and dielectric study of Bi0.5Na0.5TiO3 ceramics synthesized with precursors obtained by the sol-gel method and doped with lanthanum. *AIP Advances, 11,* 65020. https://doi.org/10.1063/5.0051792

Shohag, S.M.A.U., Franco, L., Tippur, A., Mohan, S., Rahman, M.W. & Uddin, M.J. (2024). Enhanced piezoelectric nanogenerators with Sr-doped lanthanum cobaltite (La1-xSrxCoO3) and multiwalled carbon nanotubes for energy harvesting. *ACS Applied Engineering Materials, 2,* 2842-2855. https://doi.org/10.1021/acsaenm.4c00503

Troyanchuk, I.O., Lobanovsky, L.S., Khalyavin, D.D., Pastushonok, S.N. & Szymczak, H. (2000). Magnetic and magnetotransport properties of Co-doped manganites with perovskite structure. *Journal of Magnetism and Magnetic Materials, 210,* 63-72. https://doi.org/10.1016/S0304-8853(99)00620-4

Yamada, I., Fujii, H., Takamatsu, A., Ikeno, H., Wada, K., Tsukasaki, H., Kawaguchi, S., Mori, S. & Yagi, S. (2017). Bifunctional oxygen reaction catalysis of quadruple manganese perovskites. *Advanced Materials, 29,* 1603004. https://doi.org/10.1002/adma.201603004

Yousif, N.M., Makram, N. & Wahab, L.A. (2021). Structural, dielectric, and magnetic properties of LaCo0.2Mn0.8O3 and La2CoMnO6 perovskite materials. *Journal of Sol-Gel Science and Technology, 98*, 238-251. https://doi.org/10.1007/s10971-021-05502-4

Zeng, Z., Xu, Y., Zhang, Z., Gao, Z., Luo, M., Yin, Z., Zhang, C., Xu, J., Huang, B., Luo, F., Du, Y. & Yan, C. (2020). Rare-earth-containing perovskite nanomaterials: design, synthesis, properties and applications. *Chemical Society Reviews, 49,* 1109-1143. https://doi.org/10.1039/C9CS00330D

Zhou, G., Jiang, F., Zang, J., Quan, Z. & Xu, X. (2018). Observation of superconductivity in the LaNiO3/La0.7Sr0.3MnO3 superlattice. *ACS Applied Materials & Interfaces, 10,* 1463-1467. https://doi.org/10.1021/acsami.7b17603